Sub-Doppler spectroscopy of atoms excited in the regime of Rabi oscillations in a thin gas cell

Nicolò Beverini [a], Azad Ch. Izmailov [b]

[a] *Dipartimento di Fisica dell'Università di Pisa, and CNISM, unità di Pisa, largo B. Pontecorvo 3, I 56127 Pisa, Italy*

[b] *Institute of Physics, Azerbaijan National Academy of Sciences, H. Javid av. 33, Baku, Az-1143, Azerbaijan*

Abstract

We carried out theoretical investigation about velocity-selective atomic excitation on long –lived (metastable) levels of an atomic vapour in a thin cell by a monochromatic laser beam, running in the normal direction. The regime of coherent Rabi oscillations is considered on the light-induced transition from a sublevel of the ground quantum term to a metastable atomic level. On the basis of density matrix equations for the two-level system, we analyzed the atomic population density of the metastable level, when the sample is irradiated by resonant monochromatic laser beam with an annular cross-section versus atomic velocities and versus the detuning, the amplitude, and the geometry of the laser beam. It is shown that, in the center of the annular region, it can be obtained a population distribution on the metastable level as a function of the laser detuning, characterized by a sharp narrow resonance profile, whose width is reduced with respect to the thermal Doppler width roughly by the ratio between the diameter of the irradiated region and the inner thickness of the cell. We suggest high-sensitive schemes, in order to detect these sub-Doppler resonances, by probing the population of the metastable state with a second laser beam, resonant with a transition leaving from the metastable level The case of $^1S_0 \rightarrow {}^3P_1$ spin-forbidden transition of *Ca* is discussed in more detail..

PACS: 42.62.Fi; 42.60.Lh
Keywords: Sub-Doppler spectroscopy; Thin cell; Rabi oscillations; Frequency standard

1. Introduction

Efficient methods of sub-Doppler optical spectroscopy are very important both for the precision analysis of atomic (or molecular) structure and for the realization of accurate frequency standards [1]. Recently two types of sub-Doppler resonances have been discovered and investigated, which appear on the central frequencies of the absorption profile of a rarefied atomic sample irradiated by a frequency swept monochromatic laser beam with a radius R, when it is contained in a cell whose inner thickness l is much smaller than R [2-8]. These non-trivial resonances are due to the velocity selective destruction in the collisions against the cell walls of light-induced atomic quantum state populations. Thus, narrow resonances, caused by the Dicke effect, appear on the absorption profile in a gas cell with a very small thickness l, comparable or even shorter than the laser optical wavelength λ [5-8]. From the analysis of this kind of resonances is especially interesting for obtaining information on atom-surface interactions [9]. A second kind of non-trivial sub-Doppler features may appear also in comparatively longer cells (where $l \gg \lambda$), because of the perturbation of the population of the ground quantum term sublevels by optical pumping [2-4,6]. This effects was theoretically predicted in ref. [2], and subsequently observed and analysed in experiments with the cesium vapour in thin cells whose inner thicknesses ranged from 10 μm to 1 mm [3,6]. A review of the technique, its achievements and its applications to high-resolution laser spectroscopy is presented in paper [4].

All mentioned resonances are direct manifestations of the radiative relaxation of the levels and of the corresponding optical coherences. Sub-Doppler spectral structures can be produced also in a different way as an effect of velocity selection of atoms (or molecules), when the radiative damping of the light-excited state is negligible in comparison with its relaxation rate due to the atomic (or molecular) collisions with the cell walls. This is the case of many atoms and molecules, when the laser radiation is resonant with a forbidden transition that connects a sublevel of the ground state to a sufficiently long-lived (metastable) level [10]. Indeed, the radiative life-time may be much longer than the free flight time ($10^{-3}-10^{-5}$ s) of atoms (molecules) in a rarefied gas, moving at the thermal speed u in a cell with a transversal dimension of the order of some cm. The collisions against the cell walls interrupt the interaction between such an atom and the resonant radiation. Thus, in the gas cell with a small inner thickness $l<<R$, only atoms with a sufficiently small longitudinal velocity component $|v_z|<(l/R)u<<u$ can interact with the laser beam for a time long enough in the regime of coherent Rabi oscillations [1] to be efficiently excited to the metastable level. As a consequence, the contribution of the Doppler broadening to the width of the spectral resonance will be reduced roughly by a factor *R/l,* which can be very large. This effect may be exploited both for high-resolution spectroscopy and for laser frequency stabilization.

In the present work we will theoretically investigate this process of atomic velocity selection on long-lived excited quantum level in a thin cell, when the atomic sample is irradiated in the normal direction by a resonance monochromatic laser beam. With the formalism of density matrix equations for a two-level system, we will calculate the stationary population of excited atoms versus the atomic velocity, the laser frequency and the laser intensity. The calculus will be performed, considering an annular laser beam profile (Fig. 1), and the solution will be discussed as a function of the beam spatial parameters. A high-sensitive method for recording the narrow sub-Doppler resonance, caused by the optical selection of excited atoms with small velocity projections $|v_z|<(l/R)u<<u$, is suggested. In particular, the cases will be considered of $^1S_0 \rightarrow {}^3P_1$ intercombination transition of calcium (λ=657 nm).

2. Basic equations

We consider a rarefied atomic gas, confined in a thin cell with an inner thickness l, and irradiated by a monochromatic laser beam with an annular spatial profile (with inner radius r_0 and external radius $R>>l$). The beam is propagating along the z axis, orthogonally to the plane-parallel walls of the cell (Fig.1). We will suppose that the laser intensity is uniform in the irradiated volume. Then, the beam electric field is described in cylindrical coordinates r and z by the following formula:

$$\boldsymbol{Q}(z,r,t)=\frac{1}{2}\boldsymbol{E}\cdot\eta(R-r)\cdot\eta(r-r_0)\cdot\exp\left[i(\omega t-kz)\right] + \text{c.c.}, \qquad (1)$$

where $\boldsymbol{E}=E\boldsymbol{e}$, E and $\boldsymbol{e}$ are the amplitude and the unit polarization vector of the beam, ω is the laser (angular) frequency, $k=\omega/c=2\pi/\lambda$ is the wave-number, and $\eta(x)$ is the step function ($\eta(x)$=1 for $x\geq 0$ and $\eta(x)$=0 for $x<0$).

We assume that the beam frequency ω is close to the centre ω_0 of an electric dipole transition $a\rightarrow b$ between the sublevel a of the ground quantum term and a metastable excited state b of atoms. We consider the atomic density in the cell sufficiently low, so that

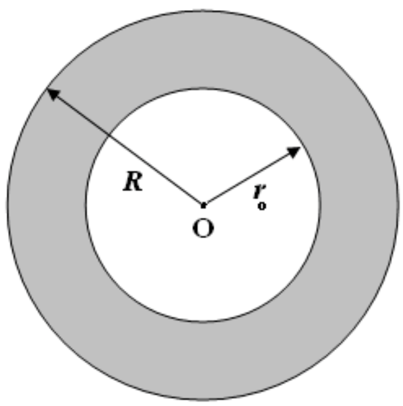

Fig.1. Irradiation of the thin gas cell (in the normal direction) by the monochromatic laser beam, having the ring-shaped cross-section with the external radius R and the inner radius r_0.

interatomic collisions can be neglected. Light pressure effects on atoms are not taken into account.

We will analyse the situation when the lifetime of the excited level *b* is much longer than the characteristic transit time *R/u* of particles moving with the most probable speed *u* across the laser beam of Eq.(1). We will not take into account the radiative relaxation of the excited level *b*.

Under these conditions, the interaction of the laser beam Eq.(1) with the atoms in the cell is described in terms of the elements of the density matrix of the optical coherence ρ_{ab} and populations ρ_a and ρ_b of levels *a* and *b* [11] by the following system of equations:

$$\rho_a + \rho_b = N \cdot F(\boldsymbol{v}) ,$$

$$\frac{\partial \rho_b}{\partial t} + \boldsymbol{v} \cdot \frac{\partial \rho_b}{\partial \boldsymbol{r}} = -\frac{1}{2} i g \cdot \rho^*_{ab} \cdot \exp\left[i\left(\delta t - kz\right)\right] + \text{c.c.},$$

$$\frac{\partial \rho_{ab}}{\partial t} + \boldsymbol{v} \cdot \frac{\partial \rho_{ab}}{\partial \boldsymbol{r}} = \frac{1}{2} i g \cdot (\rho_b - \rho_a) \exp\left[i\left(\delta t - kz\right)\right], \quad (2)$$

where *N* is the density of atoms in the ground state *a* in the absence of the laser beam, $F(\boldsymbol{v})$ is the Maxwell distribution on atomic velocities $\boldsymbol{v}$, $g=(\boldsymbol{Ed})/\hbar$ is the Rabi frequency, $\boldsymbol{d}$ is the matrix element of the dipole moment for the transition $a \to b$, and $\delta = (\omega - \omega_0)$ is the frequency detuning. Eqs.(2) must be integrated by the boundary conditions, which depend on the features of the atomic collisions with the walls of the cell. According to previous investigations [2-6], for a thin cell with a macroscopic thickness $l >> \lambda$, we may assume that equilibrium distributions for both atomic velocities and populations of quantum levels are established due to such collisions. Thus, we assume that the density matrix elements ρ_b and ρ_{ab} vanish on the cell walls. Under such conditions, we obtain from Eqs.(2) the following expression for the population $\rho_b^{(0)}$ of excited atoms on the axis of the laser beam (Fig.1; z =0 and z =l are the coordinates of inner plane-parallel cell walls):

$$\rho_b^{(0)} = N \cdot F_l(v_z) \cdot F_t(v_t) \cdot g^2 \cdot \Omega^{-2} \cdot [\beta(z, v_z, v_t) \cdot \eta(v_z) + \beta(l - z, -v_z, v_t) \cdot \eta(-v_z)], \quad (3)$$

where

$$\beta(z, v_z, v_t) = \sin^2\left[\frac{\Omega}{2}\left(\frac{z}{v_z} - \frac{r_0}{v_t}\right)\right] \cdot \eta\left(\frac{z}{v_z} - \frac{r_0}{v_t}\right) \cdot \eta\left(\frac{R}{v_t} - \frac{z}{v_z}\right) + \sin^2\left[\frac{\Omega \cdot (R - r_0)}{2 \cdot v_t}\right] \cdot \eta\left(\frac{z}{v_z} - \frac{R}{v_t}\right), \quad (4)$$

$\Omega = \left[g^2 + \left(\delta - k v_z\right)^2 \right]^{1/2}$, and v_z and v_t are the values respectively of the longitudinal and transversal (radial) components of the atomic velocity $\boldsymbol{v}$, characterized by the Maxwell equilibrium distributions:

$$F_l(v_z) = \pi^{-1/2} \cdot u^{-1} \cdot \exp(-v_z^2 \cdot u^{-2}) ,$$

$$F_t(v_t) = 2 \cdot v_t \cdot u^{-2} \cdot \exp(-v_t^2 \cdot u^{-2}) . \quad (5)$$

According to Eqs.(3)-(5), only excited atoms, moving in the cell in radial direction with longitudinal velocity component v_z close to zero, may reach the region around the centre of the laser beam (Fig.1). During the transit of these atoms through the irradiated region, coherent Rabi oscillations occur between the two levels a e b.

The averaged population density of excited atoms on the axis of the beam is calculated as:

$$n_b = \int_{-\infty}^{+\infty} P_b(v_z) dv_z , \quad (6)$$

with

$$P_b(v_z) = l^{-1} \int_0^\infty \left[\int_0^l \rho_b^{(0)}(z, v_z, v_t) dz \right] dv_t . \quad (7)$$

3. Velocity selection of excited atoms

When a Doppler broadened spectral line is irradiated by a monochromatic radiation detuned by δ from the centre of the resonance, the distribution of excited atoms as a function of the longitudinal velocity component v_z is described by a narrow resonance with a width corresponding to the homogeneous transition linewidth and with the maximum in the neighbourhood of the value $v_z = \delta / k$ [1]. Fig.2 shows the resonance values $\tilde{P}_b$ that we obtain for the function P_b in Eq.(7) at $v_z = \delta / k$, versus the Rabi frequency *g*. In the calculation presented in this chapter and in the following one we will use the numerical values for the parameters that correspond to the physical case of the intercombination *Ca* transition $^1S_0 \rightarrow {}^3P_1$ (λ=657 nm) in a thin cell with the inner thickness *l*=10μm, irradiated by a laser beam with outer radius *R*=2.5 cm.

Curves 1 and 2 in Fig.2 correspond to the atoms with zero velocity *z*-component. In this case we find the following expression for $\tilde{P}_b$ when v_z=0:

$$\tilde{P}_b(v_z = 0) =$$

$$\frac{N}{2\sqrt{\pi}\,u}\left\{1 - \int_0^\infty F_t(v_t) \cdot \cos\left[\frac{g \cdot (R - r_0)}{v_t}\right] dv_t\right\}. \quad (8)$$

The fraction of excited atoms with v_z=0 on the axis of the laser beam is given by $s_b = (\pi^{1/2} u / N)\tilde{P}_b(v_z = 0)$. According to the formula (8) (curves 1 and 2 in Fig. 2), this fraction reaches a maximum value $s_b \approx 0.677$ for $g(R - r_0)/u \approx 2.65$. Thus, in our case, because of Rabi oscillations, on the central axis of the beam the number of excited atoms is approximately two times larger than the number of atoms in the ground state *a* of the same velocity class. For the largest saturation value (in our case for $g(R - r_0)/u \geq 20$) in condition of null detuning (δ=0) the number of atoms with v_z=0 in the ground state and in the excited state are approximately equal (curves 1 and 2 in Fig.2).

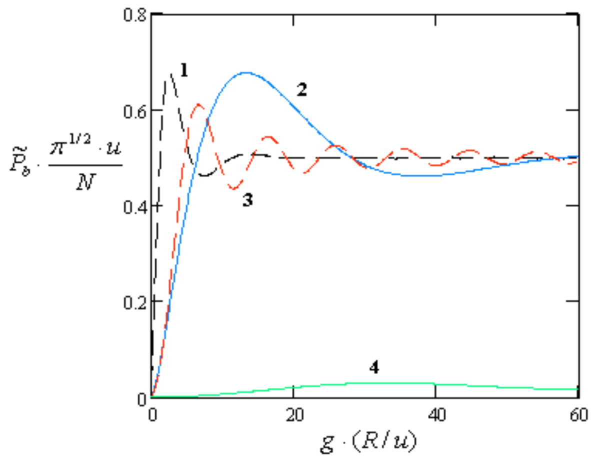

Fig.2. The resonance value $\tilde{P}_b = P_b(v_z = \delta / k)$ versus the Rabi frequency *g* (in units of the characteristic transit relaxation *u/R*), when *kl*=100, *R/l*=2500, $r_0 / R = 0$ (1,3), *and* 0.8 (2,4), $\delta / (ku) = 0$ (1,2) *and* $6 \cdot 10^{-4}$ (3,4).

Curves 3 and 4 in Fig.2 were calculated for a sufficiently large value of the frequency detuning, so that $|v_z| = |\delta| / k > (l / R)u$. If the laser beam has no hole in the centre (r_0=0), we obtain from Eqs. (3)-(5),(7) the following expression for $\tilde{P}_b = P_b(v_z = \delta / k)$, for large detuning $|\delta|$:

$$\tilde{P}_b \approx 0.5 \cdot N \cdot F_l\left(\frac{\delta}{k}\right) \cdot \left[1 - \left(\frac{|\delta|}{g \cdot k \cdot l}\right) \times \right.$$
$$\left. \times \sin\left(\frac{g \cdot k \cdot l}{|\delta|}\right)\right]. \quad (9)$$

The function $\tilde{P}_b(g)$ in Eq.(9) undergoes oscillations with a characteristic period $\Delta g = 2\pi|\delta|(kl)^{-1}$ as a function of the Rabi frequency *g* (this is particularly evident for curve 3 in Fig.2). Indeed the value $g / \Delta g = (gl)(2\pi|v_z|)^{-1}$ determines the effective number of Rabi oscillations between the two levels *a* e *b*, which occur in atoms with $v_z = \delta / k$ during their flight time $l|v_z|^{-1}$ between the plane-parallel walls of the cell, if r_0=0.

When the central black hole in the beam profile has a radius r_0>>l (curve 4 in Fig. 2), then the axis of this beam (Fig.1) is reached only by the excited atoms with longitudinal velocity $|v_z| \le v_t(l/r_0)$, where v_t is the corresponding transversal velocity. Therefore, if r_0>>l, the function $\widetilde{P}_b(\delta)$ decreases by increasing the frequency detuning $|\delta|$ much faster than in the case when r_0=0.

4. Sub-Doppler resonances

Fig.3 shows the dependence of the population density n_b Eq.(6) of excited atoms (on the central axis of the laser beam) on the frequency detuning δ. This is a symmetric curve with the centre in the point δ=0.

We see that, for sufficiently low intensities of the laser radiation, the characteristic width Δ, defined as the full width at half maximum (FWHM), of such a resonance $n_b(\delta)$ is at least by 3 orders of magnitude smaller than the characteristic Doppler broadening ku of the atomic gas in the cell. Increasing the Rabi frequency g leads to increase both the amplitude $A = n_b(\delta = 0)$ and the width Δ of the curve $n_b(\delta)$, which are essentially determined also by the width $(R - r_0)$ of the ring-shaped cross-section of the laser beam (Figs. 3, 4). Indeed, the degree of the excitation of atoms at r=0 is characterized by the parameter $g(R - r_0)/u$, where $(R - r_0)$ is the radial width of the annular shape of the laser beam (Fig.1). In particular, we observe a reduction of the field broadening of the curve $n_b(\delta)$ when the difference $(R - r_0)$ decreases. This is particularly evident with respect to the case of r_0=0 (no hole in the radiation beam) (Fig.4b). Really, if r_0=0, an effective excitation of atoms with velocity component $|v_z| \le gl$ takes place, which occurs during their transit time $(l/|v_z|)$ between the plane-parallel walls of the cell.

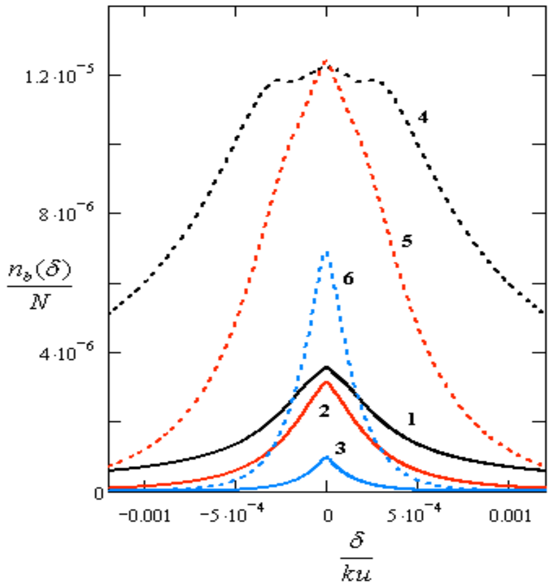

Fig. 3. The population n_b of the excited level b (in units of the atomic density N) versus the frequency detuning δ (in units of the Doppler broadening ku), when kl=100, R/l=2500, r_0/R=0 (1,4), 0.2 (2,5) and 0.8 (3,6), $g\cdot(R/u)$=1^0(1-3) and 3 (4-6).

Therefore, when r_0=0 (curve 1 in Fig.4b), we observe a significant rise of the width Δ and a flattening of the resonance profile $n_b(\delta)$ by increasing the Rabi frequency g,. At the contrary, if r_0>>l, the residual Doppler broadening for the collection of excited atoms on the axis of the cell is restricted by a comparatively small value of the order of $ku(l/r_0) << ku$. We outline that, for sufficiently low values of the Rabi frequency (gR/u≈1), the width Δ becomes close to $(l/2R)ku = 2\cdot10^{-4}ku$ (curve 2 in Fig.4b), which is a factor ≈$1.2\cdot10^{-4}$ narrower than the Doppler FWHM of the transition, given by $2\cdot\sqrt{\ln 2}\cdot ku$. The amplitude A of the resonance curve $n_b(\delta)$, as a rule, increases with growth of the radius difference $(R - r_0)$ (Fig.4a), due to a lower selection of the velocity components $|v_z|$ of excited atoms. However, in condition of strong saturation, owing to features of the Rabi oscillations, it is possible that a higher amplitude A corresponds to a smaller difference $(R - r_0)$ (see, for example, curves 1 and 2 in Fig.2).

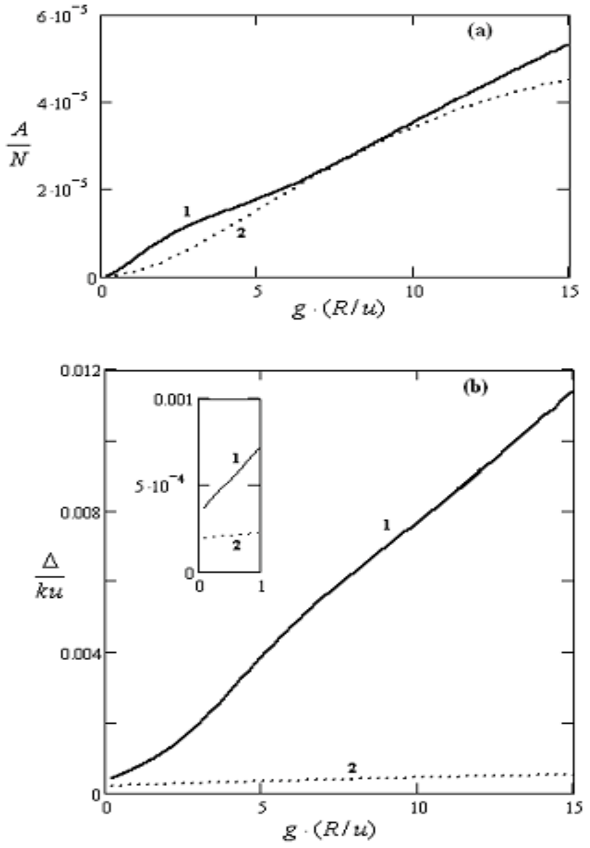

Fig.4. Dependence of the amplitude A (a) and the FWHM Δ (b) of the population spectral distribution $n_b(\delta)$ (like Fig.3) on the Rabi frequency g (in units of the characteristic transit relaxation u/R) when kl=100, R/l=2500 and r_0/R=0 (1) and 0.8 (2). The inset in (b) presents the dependence $\Delta(g)$ for sufficiently small Rabi frequencies.

It is important to note the very sharp line profile around the centre of given resonances (in particular curves 3 and 6 in Fig.3). The sharpness of the profile may be characterized by the parameter $Q = \frac{\Delta^2}{8n_b(0)} \left| \frac{\partial^2 n_b(\delta)}{\partial \delta^2} \right|_{\delta=0}$, proportional to the normalized value of the second derivative of the function $n_b(\delta)$ in the point δ=0, which is equal to 1 in the case of a Lorentzian shaped curve and equal to $log2$≈0.693 for a Gaussian one. We have evaluated this parameter Q for the sub-Doppler profile for different values of r_0 and g, finding values between 2.5 and 4.2, almost when $gR/u \leq 3$ and $r_0 \geq 0.4Rl$ (and kl=100) as in Figs. 3 and 4. The larger value Q allows an more effective frequency locking of the laser source to the resonance centre through the usual frequency modulation technique, when the transition is used as a frequency reference.

The calculations in sections 2-4 of this work were performed considering a non-degenerate two-level system. However it is straightforward to generalize the results for nonzero angular momenta of levels a and b considering linear or circular polarization of the monochromatic laser beam. Indeed, the radiation will interact with the collection of independent transitions between the Zeeman sublevels of a and b [1].

We did not consider very small values of the Rabi frequency $g \ll u(R-r_0)^{-1}$, when the effective excitation on the transition $a \to b$ takes place only for negligible fraction of very slow atoms. For these atoms, effects related to the radiative damping of the long-lived level b should be possible, which is not taken into account in our calculations.

We have also assumed that the intensity of the laser beam Eq.(1) is constant on its ring-shaped cross-section. This does not correspond to a real experimental condition. Therefore, in order to analyse the experimental data, it will be necessary to average over the effective value of the Rabi frequency g on the laser beam cross-section.

The use of annular shaped geometry for laser beam was already discussed in an experimental work [12] for detection of Cs atoms flying under grazing incidence to walls of the thin vapour cell.

5. Detection schemes

It should be possible to detect the sub-Doppler resonances simply monitoring the fluorescence due to the radiative decay of the metastable atoms in the central region of the laser beam (Fig.1). The behaviour of absorption and fluorescence spectrum in extremely thin vapour cell was already extensively discussed in ref [13], with reference to D_2 transition in rubidium. We will here calculate the expected resonance signal magnitude for ${}^1S_0 \to {}^3P_1$ 657 nm calcium transition in an experimental apparatus where the fluorescence coming from a cylindrical volume around the axis with radius r_1=5 mm is focalized over the photodetector (with a collection solid angle $\varepsilon \approx$ 1/10 steradian). In the conditions of the curve 6 in Fig. 3 (r_0 /R=0.8 and $g \cdot R / u$ =3), the population density of the excited state on the laser beam axis is at resonance $n_b(0) \approx 6 \cdot 10^{-6}$ N. We assume an atomic calcium vapour density N=10^{12} atoms/cm^3 which corresponds to the saturated vapour density at 445 °C (in this condition u=545 m/s and the collisional free mean path is longer than 1 m). The number of the fluorescence photons coming out from the considered volume in one second is then:

$$\pi l r_1^2 n_b(0) \cdot \frac{\varepsilon}{4\pi} \cdot \frac{1}{\tau} \approx 10^5 \text{ photon/s},$$

where τ = 0.34 ms is the lifetime of $^3P_1$ of calcium [14]. Signal-to noise ratio will be quite poor, also for the unavoidable background due to the light scattered from the pumping beam.

More efficient schemes, valid also for transitions with very long metastable level lifetime, are possible, by using a second probe laser, which is resonant with a transition leaving from the metastable level. It is convenient to direct this additional radiation coaxial to the pumping beam inside the dark hole of its annular shape (Fig.1). Then, due to the spatial separation of these light fields in a gas cell, the probe radiation will not effect on the optical velocity selection of metastable atoms induced by pumping beam. In this case the number of collected fluorescence photons is simply limited by the diffusion rate of metastable atoms from the pumping region to the detection volume ($\approx 10^5$ s^{-1} in our geometry). Moreover, it is possible in this case to use a phase sensitive detection technique by frequency modulating the pumping beam, allowing the discrimination of the fluorescence photons from the scattered ones. A great improvement of signal-to noise ratio can be given, if a close transition leaving from the metastable level is available, which does not destroy metastable level population.

In the case of the metastable $(4s4p)^3P_1$ calcium level, suitable transitions can be: the 612.2 nm transition leading to $^3S_1$, 443.5 nm transition leading to $^3D_2$, or the 430 nm transition leading to $(4p_2)^3P_0$. The use as probe transition of the closed transition $(4s4p)^3P_1 \to (4p_2)^3P_0$ at 430 nm, do not destroy the metastable level population, and can recycle a single metastable atom more than 1000 times during its crossing the probe beam. Considering again the condition of the curve 6 in Fig. 3 ($g{\cdot}R/u$=3, r_0=2 cm, $n_b(0) \approx 6 \cdot 10^{-6} N$), we estimate a signal on the photodetector at the resonance:

$$k_c \frac{\varepsilon}{4\pi} \frac{n_b(0)\, V}{r_1 / u} = \frac{k_c}{4} \varepsilon u\, n_b(0)\, r_1 l \approx 4 \cdot 10^9 \text{ photons/s}$$

where r_1=5 mm is the radial dimension of the probe beam, $V = \pi \cdot r_1^2 l$ is the probed volume, l=10 μm, r_1 / u is the diffusion time of an atom through the probe beam, N=10^{12} cm^{-3} is the atomic density, ε=1/10 sterad is the collection angle, and k_c is the recycle factor of the probing transition (1000 for the considered transition). From this result we obtain a shot noise limit for the relative frequency stability of a laser oscillator locked to this resonance profile below $10^{-13}\sqrt{T}$, where T is the integration time.

The preparation of shallow cells for containing the alkaline earths can be a hard job, requiring sophisticated techniques. While with alkali atoms, in particular *Rb* and *Cs*, it is possible to operate near room temperature or only slightly above, thus allowing the use of Pyrex or quartz cells [3,4,6], alkaline-earth elements at the temperatures needed to have suitable vapour density are chemically strongly reactive, restricting the choice of possible transparent materials. Anyway, the realization of a sapphire cell should be possible by using ultrasound digitally controlled milling-machin [15] and a high vacuum manipulation utility.

6. Conclusions

We have shown possible selective excitation of atoms with the small velocity projection $|v_z| \le (l/R)u$ along the axis of a thin cell with inner thickness l in the regime of coherent Rabi oscillations between the quantum levels of the resonance optical transition induced by this monochromatic beam of radius $R >> l$, running in the normal direction. We have demonstrated that the dependence of the population of the excited atoms on the laser frequency detuning presents a very narrow sharp resonance profile around the centre of the quantum transition, because the contribution of the Doppler broadening to the width of this resonance can be reduced by a factor of the order of $2R/l >> 1$. At a fixed radius of the thin cell, the narrowest sub-Doppler resonances can be obtained by using an annular geometry of the laser beam .

It is important to outline that in all previous papers, concerning the spectroscopy in a thin gas cells [2-9], only such situations were considered, when the natural width of the resonance optical transition was much larger than the inverse of the characteristic transit time of atoms across laser beams (in this work determined by u/R). In this work we are in the opposite situation, and , it is therefore possible to detect essentially narrower sub-Doppler resonances. Thus such sharp narrow resonances in thin gas cells can be usefully exploited for building effective compact optical frequency references with low power requirements.

High-sensitive method of recording these sub-Doppler resonances in the fluorescence of atoms has been suggested. We have analysed, in particular, the case of the $^1S_0 \rightarrow {}^3P_1$ intercombination *Ca* transition (λ=657 nm) in a thin cell with the calcium vapour. However the suggested method is quite general, and do not apply only to the case of alkali-earth atoms and to electric dipole transition. It could also be applied to any transition from the ground state and a metastable level like, for example, the quadrupole electrical strontium transition $^1S_0 \rightarrow {}^1D_2$ at 457 nm, or the magnetic dipole $^3P_0 \rightarrow {}^3P_1$ transition inside the ground state multiplet of *Pb* at 1278.9 nm.

The experimental study of this velocity selective effect can also produce valuable information on atom-surface interactions [9], by studying the collisional shifts and shape changes of these very narrow sub-Doppler resonances. Particularly interesting should be the possible extention of this kind of investigation to very thin gas cells with the microscopic thickness $l < \lambda$.

References

[1] W. Demtröder, Laser Spectroscopy, Heidelberg, Springer, Berlin, 1996.

[2] A.Ch. Izmailov, Laser Physics 2 (1992) 762-763; Optics and spectroscopy 74 (1993) 25-29.

[3] S. Briaudeau, D. Bloch, M. Ducloy, Europhysics Letters 35 (1996) 337-342.

[4] A. Ch. Izmailov, (report at ICONO'2007) Proc. of SPIE 6727 (2007) 67270B.

[5] B. Zambon, G. Nienhuis, Optics Communications 143 (1997) 308-314.

[6] S. Briaudeau, D. Bloch, M. Ducloy, Phys. Rev. A 59 (1999) 3723-3735.

[7] D. Sarkisyan, D. Bloch, A. Papoyan, and M. Ducloy, Optics Communications 200 (2001) 201-208.

[8] G. Dutier, A. Yarovitski, S. Saltiel, A. Papoyan, D. Sarisyan, D. Bloch, and M. Ducloy, Europhysics Letters 63 (2003) 35-41.

[9] D. Bloch, M. Ducloy, Advances in atomic, molecular, and optical physics 50 (2005) 91-154.

[10] A. A. Radtsig, B. M. Smirnov, Reference data on atoms, molecules and ions, Springer , New York , 1985.

[11] S. Stenholm, Foundations of Laser Spectroscopy, Wiley, New York, 1984.

[12] S. Briaudeau, S. Saltiel, J.R.R. Leite, M. Oria, A. Bramati, A. Weis, D. Bloch, and M. Ducloy, J. Phys. IV France 10 (2000) Pr8-145.

[13] D. Sarkisyan, T. Varzhapetyan, A. Sarkisyan, Yu. Malakyan, A. Papoyan, A. Lezama, D. Bloch, and M. Ducloy, Phys. Rev. A 69 (2004) 065802.

[14] G. Wilpers, C. W. Oates, S. A. Diddams, A. Bartels, T. M. Fortier, W. H. Oskay, J. C. Bergquist, S. R. Jefferts, T. P. Heavner, T. E. Parker, and L.Hollberg, Metrologia 44 (2007) 146–151.

[15] A. Bertolini, N. Beverini, G. Del Lago, R. De Salvo, F.,Fidecaro, F. Francesconi, M. Francesconi, G. Omiccioli: 5-axis CNC ultrasonic cutting machine: design and preliminare test, LIGO Technical Note T020198R-00-R (2002) http://www.ligo.caltech.edu/docs/T/T020198-00/

[a] E-mail: beverini@df.unipi.it

[b] E-mail: azad57@mail.ru